Attosecond-magnetic-field-pulse generation by electronic currents in bichromatic circularly polarized UV laser fields

Kai-Jun Yuan* and André D. Bandrauk†

Laboratoire de Chimie Théorique, Faculté des Sciences, Université de Sherbrooke, Sherbrooke, Québec, Canada, J1K 2R1

(Received 3 August 2015; published 2 December 2015; publisher error corrected 3 March 2016)

Attosecond-magnetic-field-pulse generation is simulated from numerical solutions of time-dependent Schrödinger equations for oriented H_2^+. Two schemes with high frequency co- and counter-rotating bichromatic $\omega_2 = 2\omega_1$ circularly polarized UV laser pulses are investigated. Results show that comparing to single color processes, stronger induced localized magnetic fields **B** at the molecular center O ($\mathbf{r} = 0$) are obtained with attosecond duration. This is attributed to frequent recollision and to interference effects of two pathways in photoionization. The induced magnetic fields are shown to be sensitive to (i) the helicity of the combined laser pulses due to different recollision laser-induced electron trajectories and currents, and (ii) also the carrier envelope phases of the combined attosecond laser pulses. The sensitivity of recollision to bichromatic pulses thus allows one to control the induced magnetic-field-pulse generation.

DOI: 10.1103/PhysRevA.92.063401 PACS number(s): 33.80.Rv, 33.20.Lg, 42.50.Hz

I. INTRODUCTION

Optically induced magnetic fields as tools for investigations of new phenomena, such as molecular paramagnetic bonding [1], nonequilibrium electronic processes [2], demagnetization processes [3], and optical magnetic recording [4] have attracted considerable attention in past years. Photoinduced magnetization induced by circularly polarized light, i.e., the inverse Faraday effect (IFE) arising from spin-orbit and crystal field splitting [5] has been well studied. IFE has also been shown to coherently control spin dynamics in magnets with circularly polarized femtosecond laser pulses [6]. Recently it has been shown that laser-induced magnetic fields can be efficiently generated in molecules from electronic ring currents. By quantum-chemical numerical simulations unidirectional constant valence-type electronic currents and associated static magnetic fields [7] can be generated by means of circularly polarized π UV laser pulses resonant with degenerate π orbitals. It is found that the laser-induced magnetic fields can be much larger than those obtained by traditional static field methods [8]. Linearly polarized laser pulses can also induce excited ring currents by controlling the rotation direction of π electrons in planar or nonplanar aromatic molecules [9]. The driving laser pulses can be optimized as well by optimal control theory [10].

Advances in synthesizing ultrashort intense pulses [11,12] offer the possibility of visualizing and controlling electrons on their natural attosecond (1 as $= 10^{-18}$ s) time scale and subnanometer dimension, e.g., [13–16]. To date the shortest *linearly* polarized single pulse with duration of 67 as has been produced from high-order harmonic generation (HHG) with a few cycle linearly polarized intense infrared laser field in atoms [17]. The mechanism of HHG with these pulses is due to a recollision of the electron with the parent ion [18] or neighbors at large distance as in dissociated molecules [19]. Intense circularly polarized attosecond pulses are drawing increasing attention in laser science such as the generation of plasma filaments in air [20]. We have proposed to create "spinning" continuum electrons which can be generated and remain localized on subnanometer molecular dimensional scales [21,22]. As a result, time-dependent circular coherent electron wave packets (CEWPs) and currents are created in the continuum, which are the source of intense time-dependent internal magnetic fields generated on an attosecond time scale. The induced attosecond magnetic fields have been shown to be a function of the pulse wavelength and duration [23], thus offering new tools for ultrafast magnetism generation [24,25].

In the present work we investigate attosecond-magnetic-field generation and electronic currents by bichromatic circularly polarized UV laser pulses. Ultrafast intense circularly polarized pulses in general do not generate HHG in atoms since spinning electrons do not recollide with parent ions [18]. Recollision can be induced in molecules dissociated to large internuclear distances [21]. It has already been shown in 1995 that co-rotating or counter-rotating intense ultrafast circularly polarized pulses will always induce recollision thus ensuring efficient HHG [26,27]. This can be readily concluded by considering a general atomic or molecular Hamiltonian $H_0(\mathbf{r})$ in the presence of a circularly polarized pulse of intensity E_0 and frequency $\bar{\omega}$ with an envelope modulated at frequency ω. The time-dependent part of the Hamiltonian is thus written as [26] [throughout this paper, atomic units (a.u.) $e = \hbar = m_e = 1$ are used unless otherwise stated]

$$V_L(\mathbf{r},t) = E_0 \cos(\omega t)[x\cos(\bar{\omega}t) + y\sin(\bar{\omega}t)] \quad (1)$$

$$= \frac{E_0}{2}\{x\cos[(\omega+\bar{\omega})t] + y\sin[(\omega+\bar{\omega})t]\} + \frac{E_0}{2}\{x\cos[(\omega-\bar{\omega})t] + y\sin[(\omega-\bar{\omega})t]\}. \quad (2)$$

Setting the resonant condition $\omega = \bar{\omega}$ results in the combination of a circularly polarized pulse of frequency 2ω and a static field of equal amplitudes $E_0/2$. Such a Hamiltonian has been previously considered for Rydberg atoms [28,29] leading to the conclusion of stable Rydberg wave packets. We have shown that the case $\omega \approx \bar{\omega}$, where $\omega + \bar{\omega}$ is a 800-nm near-IR pulse and $\omega - \bar{\omega}$ is a much lower frequency TeraHertz pulse leads to recollision and circularly polarized HHG from which one

*kaijun.yuan@usherbrooke.ca
†andre.bandrauk@usherbrooke.ca

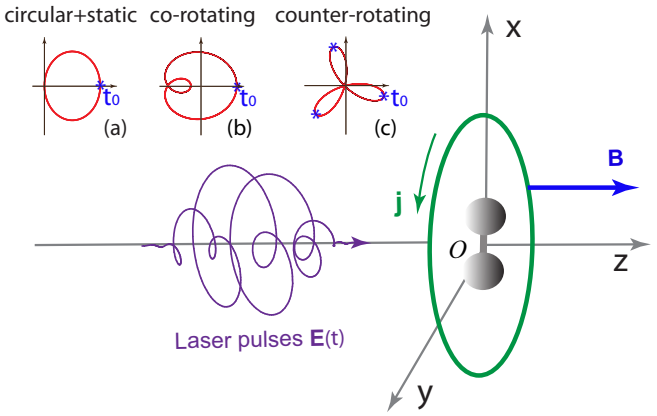

FIG. 1. (Color online) Illustrations of the laser-induced electronic currents and magnetic field generation in aligned H_2^+ by bichromatic circularly polarized attosecond UV laser pulses $\mathbf{E}(t)$. The ionizing laser pulse is polarized in the molecular (x,y) plane, propagating along the z axis. The green line **j** denotes electronic currents around the molecular center O in the laser polarization (x,y) plane. The blue line **B** indicates the induced magnetic field at the electron origin and the molecular center O, along the z axis and perpendicular to the electronic currents **j**. Inserts (red lines) are the combined bichromatic circularly polarized laser electric fields **E** for (a) a circularly polarized pulse and a static field, (b) the co-rotating, and (c) counter-rotating schemes. t_0 $(*)$ indicates the ionization time at the maximum strength of the combined fields.

can generate circularly polarized attosecond pulses [22]. The total (net) electric field for this case is illustrated in Fig. 1(a) as a shifted circularly polarized pulse which induces recollision to the atomic or molecular center. Equations (1) and (2) show that a circularly polarized laser field of frequency $\bar{\omega}$ when modulated at frequency ω can equivalently be considered as a combination of two circularly polarized fields with frequencies $\omega \pm \bar{\omega}$. Applying the unitary transformation $\mathcal{T} = \exp(-i\bar{\omega}tl_z)$, a rotation in the $+z$ direction perpendicular to the (x,y) molecular plane, Fig. 1, transforms Eqs. (1) and (2) into $\mathcal{T}^+ V_L \mathcal{T} = xE_0\cos(\omega t)$, so that the total Hamiltonian in this rotating frame of frequency $\bar{\omega}$ becomes [26]

$$H(\mathbf{r},t) = H_0(\mathbf{r}) - \bar{\omega}l_z + xE_0\cos(\omega t). \tag{3}$$

Equation (3) shows that recollision through the term $xE_0\cos(\omega t)$ as linear polarization [18] always occurs in competition with a Coriolis force $-\bar{\omega}l_z$, since the terms do not commute, $[x,l_z] \neq 0$.

The case $\bar{\omega} = 3\omega$ [Fig. 1(b)] leads to a co-rotating combination with frequencies $\omega_1 = 4\omega = 2\omega_2$, whereas $\omega = 3\bar{\omega}$ results in [Fig. 1(c)] counter-rotating fields with $\omega_2 = 4\omega = 2\omega_1$. In this case, the co-rotating scheme does not lead to recollision whereas the counter-rotating case leads to three recollisions for intense fields. The net fields in Eq. (2) easily lead to the condition that for *co-rotating* pulses, even frequency ratios $\bar{\omega} = 2n\omega$ always lead to two recollisions whereas for odd ratios $\bar{\omega} = (2n+1)\omega$ total recollisions are absent. The *counter-rotating* case, $\omega > \bar{\omega}$ always leads to recollisions, with even frequency ratios $\omega = 2n\bar{\omega}$ leading to $4n$ recollisions whereas odd frequency ratios $\omega = (2n+1)\bar{\omega}$ lead to $(2n+1)$ recollisions [30].

Such co-rotating and counter-rotating laser fields are now being adopted to produce circularly polarized HHG [31] and probe atomic and molecular structure by photoelectron momentum distributions [32]. The induced electronic currents generated by such fields exhibit a sensitivity to the field helicity. The ionized electron can re-encounter nuclei multiple times in such schemes, and as a result strong magnetic fields are generated. With time-delay bichromatic circularly polarized fields, one can also produce single attosecond pulses by gating HHG emission [33] and helical electron vortices in atomic photoionization momentum distributions [34]. Molecular ions can be pre-oriented before ionization with current orientation laser technology [35], thus enhancing such recollisions.

The paper is organized as follows. We briefly describe the computational method for solving TDSEs of aligned molecular ions H_2^+ in Sec. II. Results of induced electron currents and attosecond magnetic fields by intense bichromatic circularly polarized attosecond UV laser pulses are presented and discussed in Sec. III. Effects of pulse helicities and phases are also compared. In Sec. IV we finally summarize our findings.

II. NUMERICAL METHODS

We numerically solve the corresponding three-dimensional (3D) time-dependent Schrödinger equations (TDSE) for x-aligned H_2^+ within the static [Born-Oppenheimer approximation (BOA)] nuclear frame using cylindrical coordinates $\mathbf{r} = (\rho,\theta,z)$ with the laser polarization in the molecular plane $x = \rho\cos\theta$ and $y = \rho\sin\theta$, illustrated in Fig. 1,

$$i\frac{\partial}{\partial t}\psi(\mathbf{r},t) = \left[-\frac{1}{2}\nabla^2 + V_{en}(\mathbf{r}) + V_L(\mathbf{r},t)\right]\psi(\mathbf{r},t). \tag{4}$$

The 3D TDSE in Eq. (4) is propagated by a second-order split operator method which conserves unitarity in the time step δt combined with a fifth-order finite difference method and Fourier transform technique in the spatial steps $\delta\rho$, δz, and $\delta\theta$ [36]. The time step is taken to be $\delta t = 0.01$ a.u.=0.24 as. The spatial discretization is $\delta\rho = \delta z = 0.25$ a.u. for a radial grid range $0 \leqslant \rho \leqslant 128$ a.u. (6.77 nm) and $|z| \leqslant 32$ a.u. (1.69 nm), and the angle grid size $\delta\theta = 0.025$ radian. To prevent unphysical effects due to the reflection of the wave packet from the boundary, we multiply $\psi(\rho,\theta,z,t)$ by a "mask function" or absorber in the radial coordinates ρ with the form $\cos^{1/8}[\pi(\rho-\rho_a)/2\rho_{abs}]$. For all results reported here we set the absorber domain at $\rho_a = \rho_{max} - \rho_{abs}$=104 a.u. with $\rho_{abs} = 24$ a.u., exceeding well the field-induced electron oscillation $\alpha_d = E/\omega^2$ of the electron [23].

The radiative interaction between the laser field and the electron is described in the length gauge by

$$V_L(\mathbf{r}) = \mathbf{r}\cdot\mathbf{E}(t) = \rho\cos\theta E_x(t) + \rho\sin\theta E_y(t) \tag{5}$$

for circularly polarized pulses,

$$\begin{aligned}\mathbf{E}(t) &= \mathbf{E}_1(t) + \mathbf{E}_2(t)\\ &= Ef(t)\{\hat{e}_x[\cos(\omega_1 t+\phi_1) + \cos(\omega_2 t+\phi_2)]\\ &\quad + \hat{e}_y[\sin(\omega_1 t+\phi_1) \pm (\sin(\omega_2 t+\phi_2)]\},\end{aligned} \tag{6}$$

where the sign $\pm$ denotes co-rotating or counter-rotating, propagating in the z direction perpendicular to the molecular

(x,y) plane and $\hat{e}_{x/y}$ is the polarization direction. ϕ_1 and ϕ_2 are the carrier envelope phases (CEPs) of the pulses $\mathbf{E}_1(t)$ and $\mathbf{E}_2(t)$. A smooth $\sin^2(\pi t/n\tau)$ pulse envelope $f(t)$ for maximum amplitude E and intensity $I = I_x = I_y = c\varepsilon_0 E^2/2$ is adopted, where one optical cycle period $\tau_{1,2} = 2\pi/\omega_{1,2}$. This pulse satisfies the total zero area $\int E(t)dt = 0$ in order to exclude static field effects [11].

The time-dependent electronic current density is defined by the quantum expression in the length gauge,

$$\mathbf{j}(\mathbf{r},t) = \frac{i}{2}[\psi(\mathbf{r},t)\nabla_{\mathbf{r}}\psi^*(\mathbf{r},t) - \psi^*(\mathbf{r},t)\nabla_{\mathbf{r}}\psi(\mathbf{r},t)], \quad (7)$$

$\psi(\mathbf{r},t)$ is the exact Born-Oppenheimer (static nuclei) electron wave function obtained from the TDSE and $\nabla_{\mathbf{r}} = \mathbf{e}_\rho\nabla_\rho + \mathbf{e}_\theta\frac{1}{\rho}\nabla_\theta + \mathbf{e}_z\nabla_z$ in cylindrical coordinates. Then the corresponding *time-dependent* magnetic field is calculated using the following classical Jefimenko's equation [37]:

$$\mathbf{B}(\mathbf{r},t) = \frac{\mu_0}{4\pi}\int\left[\frac{\mathbf{j}(\mathbf{r}',t_r)}{|\mathbf{r}-\mathbf{r}'|^3} + \frac{1}{|\mathbf{r}-\mathbf{r}'|^2 c}\frac{\partial\mathbf{j}(\mathbf{r}',t_r)}{\partial t}\right] \times(\mathbf{r}-\mathbf{r}')d^3\mathbf{r}', \quad (8)$$

where $t_r = t - r/c$ is the retarded time and $\mu_0 = 4\pi \times 10^{-7}$ NA^{-2} (6.692×10^{-4} a.u.). Units of $B(\mathbf{r},t)$ are Teslas (1 T = 10^4 G).

III. RESULTS AND DISCUSSIONS

We first consider a bichromatic circularly polarized attosecond UV laser pulse with co-rotating components, i.e., two left-handed pulses. The pulse wavelengths are, respectively, $\lambda_1 = 70$ nm and $\lambda_2 = 35$ nm, corresponding to angular frequencies $\omega_1 = 0.65$ a.u. and $\omega_2 = 1.3$ a.u. We also fix CEPs $\phi_1 = \phi_2 = 0$, the pulse intensity $I = 1 \times 10^{16}$ W/cm^2, and duration $T = 5\tau_1 = 10\tau_2$ ($\tau_1 = 2\pi/\omega_1 = 2\tau_2 = 2\pi/\omega_2$) corresponding to 580 as full width at half maximum (FWHM). We choose short wavelengths λ or high frequencies ω in order to keep the radii of electronic currents of molecular dimension since such laser-induced radii are defined by $r_n \sim (2E/\omega^2)\sqrt{1+(n+1/2)^2\pi^2}$ [21]. Results show that with such intense bichromatic high frequency circularly polarized attosecond laser pulses which produce small radii currents, a magnetic field with strength $B_{co} = 0.78$ T (0.78×10^4 G) is produced at the molecular center O. We also simulate the results of induced magnetic fields B with one-color 580 as FWHM circularly polarized attosecond pulses at separate wavelengths $\lambda = 70$ nm and 35 nm. The corresponding maximum strengths of induced magnetic field at the molecular center O are smaller, $B_{\omega_1} = 0.54$ T ($0.69B_{co}$) and $B_{\omega_2} = 0.44$ T ($0.56B_{co}$). Comparing to the two-color processes, one sees that weaker magnetic fields B are induced by the single color laser pulses.

We then adopt attosecond perturbation theory [38,39] in combination with a classical laser-induced electron motion model [18,40] to describe the magnetic field generation in bichromatic fields. As shown in Eq. (7), the laser-induced electronic current j is a product of the continuum electron density (ionization probability) $\varrho = |\psi(\mathbf{r},t)|^2$ and the laser-induced velocity v (or $\nabla_{\mathbf{r}}$), i.e., $j \sim \varrho v$. The magnetic field B at O in Eq. (8) is shown to be directly proportional to the induced electronic current j and inversely proportional to the current radius r. These intense B fields are obtained with high frequency laser pulses which produce currents with small radii [21]. The time-dependent term $1/c\partial\mathbf{j}(\mathbf{r},t)/\partial t$ in Eq. (8) is usually found to be negligible, thus simplifying the induced magnetic field B to

$$B \sim \frac{j}{r} \sim \varrho\frac{v}{r} = \varrho\alpha, \quad (9)$$

which can be decomposed into two components, the ionized electron density ϱ and a ratio of the electron velocity and radius, $\alpha = v/r$ [7] [Eq. (8)].

For direct one ω_2 photon ionization processes by laser pulses, the relevant transition matrix element $\mathcal{W}^{(1)}$ can be expressed simply in the dipole form,

$$\mathcal{W}^{(1)} = \langle\psi_c|\mathbf{D}\cdot\mathbf{F}_2(\omega_2)|\psi_0\rangle = \sigma^{(1)}\mathcal{F}_2(\omega_2), \quad (10)$$

with the first-order ionization amplitude,

$$\sigma^{(1)} = \langle\psi_c|\mathbf{D}\cdot\mathbf{e}|\psi_0\rangle, \quad (11)$$

where $|\psi_0\rangle$ and $|\psi_c\rangle$ are, respectively, the initial ground state and the continuum state. $\mathbf{D}$ is the electric dipole operator. $\mathbf{F}_2(\omega_2) = \mathbf{e}\mathcal{F}_2(\omega_2) = E_0(\omega_2)e^{i\phi_1}$ is the ionizing pulse amplitude with unit vector $\mathbf{e}$ and field $E_0(\omega_2)$.

For the $\lambda_1 = 70$ nm ($\omega_1 = 0.65$ au) laser pulse, at least a two $\omega_1 + \omega_1$ photon absorption is required to ionize H_2^+. The transition matrix element reads as

$$\mathcal{W}^{(2)} = \sigma^{(2)}\mathcal{F}_1^2(\omega_1), \quad (12)$$

with the amplitude,

$$\sigma^{(2)} \sim \int dE\frac{\langle\psi_c|\mathbf{D}\cdot\mathbf{e}|\psi_n\rangle\langle\psi_n|\mathbf{D}\cdot\mathbf{e}|\psi_0\rangle}{E_{1s\sigma_g} - E_{ni} + \omega_1 + i\eta}, \quad (13)$$

where ψ_n and E_{ni} are the wave function and energy of the intermediate (virtual) electronic state and η is the level width, and laser fields $\mathcal{F}_1(\omega_1) = E_0(\omega_1)e^{i\phi_2}$. Since the energy difference between the ground $1s\sigma_g$ state and the excited $2p\pi_u$ state is $\Delta E_{\sigma\pi} = E_{2p\pi_u} - E_{1s\sigma_g} = 0.65$ a.u., a resonant excitation occurs, thus enhancing the ionization, and one obtains $B_{\omega_1} > B_{\omega_2}$.

For photoionization by bichromatic laser pulses, that is, simultaneous two $\omega_1 + \omega_1$ photon and one $\omega_2 = 2\omega_1$ photon ionization, the total transition probability is the square of the two amplitudes with an interference term of the cross products of the two one- and two-photon ionization amplitudes, that is,

$$\mathcal{W} = |\mathcal{W}^{(1)}|^2 + |\mathcal{W}^{(2)}|^2 + \mathcal{W}^{(1,2)}, \quad (14)$$

where $\mathcal{W}^{(1,2)}$ is the interference term which can be simply written as

$$\mathcal{W}^{(1,2)} = \mathcal{W}^{(1)*}\mathcal{W}^{(2)} + \mathcal{W}^{(1)}\mathcal{W}^{(2)*} = 2\sigma^{(1)}\sigma^{(2)}E_0^2(\omega_1)E_0(\omega_2)\cos(\Delta\phi), \quad (15)$$

where $\sigma^{(1)}$ and $\sigma^{(2)}$ are the one ω_2 and two $\omega_1 + \omega_1$ photon transition amplitudes corresponding to Eqs. (11) and (13) and the relative phase difference $\Delta\phi = \phi_2 - 2\phi_1$. From Eq. (9) we note that the induced magnetic field B is directly proportional to the ionization density ϱ. Since the CEP difference $\Delta\phi = 0$, i.e., $\cos\Delta\phi = 1$, the interference effect of CEWPs enhances

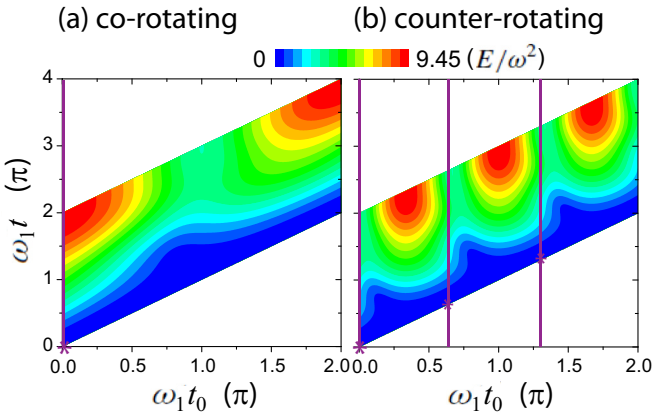

FIG. 2. (Color online) Classical electron trajectories $r(t) = \sqrt{x^2(t) + y^2(t)}$ as functions of $\omega_1 t_0$ and $\omega_1 t$ by the bichromatic circularly polarized pulses for the (a) co- and (b) counter-rotating cases with CEPs $\phi_1 = \phi_2 = 0$. Purple lines (∗) indicate the initial ionization time t_0 at maxima of electric fields; cf Fig. 1.

the ionization in Eq. (14). Comparing to single color photoionization, stronger induced magnetic fields B are thus obtained with bichromatic laser pulses $\mathbf{E}(t)$.

We next present the effects of the helicity of the ionizing circularly polarized fields on the induced magnetic field B. From Eq. (9) we note that the induced magnetic field B is also a function of the radii of the ionized electron. Figure 2 illustrates the electron trajectories $r(t) = \sqrt{x^2(t) + y^2(t)}$ as functions of $\omega_1 t_0$ and $\omega_1 t$ ($\omega_2 = 2\omega_1$) in the bichromatic circularly polarized electric fields obtained from the classical laser-induced electron motion model [18,21], where t_0 is the ionization time. We assume zero initial velocity and position of one ionized electron. The laser-induced electron displacements read [21]

$$
\begin{aligned}
x(t) = &-\frac{E}{\omega_1^2}\{\cos\omega_1 t_0 - \cos\omega_1 t - \sin\omega_1 t_0(\omega_1 t - \omega_1 t_0) \\
&+ \frac{1}{4}[\cos\omega_2 t_0 - \cos\omega_2 t - \sin\omega_2 t_0(\omega_2 t - \omega_2 t_0)]\}, \\
y(t) = &-\frac{E}{\omega_1^2}\{\sin\omega_1 t_0 - \sin\omega_1 t + \cos\omega_1 t_0(\omega_1 t - \omega_1 t_0) \\
&\pm\frac{1}{4}[\sin\omega_2 t_0 - \sin\omega_2 t + \cos\omega_2 t_0(\omega_2 t - \omega_2 t_0)]\}.
\end{aligned}
\tag{16}
$$

As illustrated in Fig. 1 the ionization mainly occurs at the time of the maximum values of the combined fields, i.e, $t_0 \approx n\tau_1 = 2n\pi/\omega_1$, $n = 0,1,2,3,\ldots$, for co-rotating and $n\tau_1/3 = 2n\pi/3\omega_1$ for counter-rotating cases. One sees in Fig. 2(a) that for a bichromatic *co-rotating* circularly polarized laser pulse, the combined field forces the ionized electron quickly far away from the molecular center, giving rise to large radii; whereas for a bichromatic *counter-rotating* case in Fig. 2(b), the electron moves around the molecular center with small radii, and multiple recollisions of the electron with its parent ion occur thus producing HHG [26,27,31]. Strong magnetic fields are therefore predicted to be generated preferentially for the counter-rotating scheme.

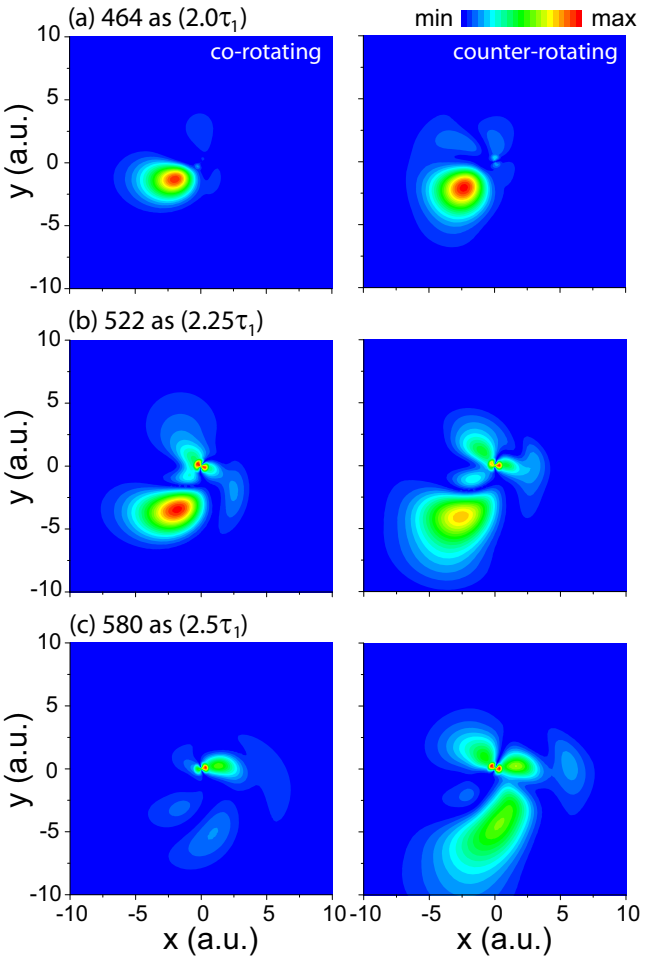

FIG. 3. (Color online) Evolution of electronic currents $j(x,y,t)$ with time t by (left column) co-rotating and (right column) counter-rotating bichromatic $I = 1 \times 10^{16}$ W/cm^2 and 580 as FWHM circularly polarized UV pulses at wavelengths $\lambda_1 = 70$ ($\omega_1 = 0.65$ a.u.) nm and $\lambda_2 = 35$ nm ($\omega_2 = 1.3$ a.u.). ($1\tau_1 = 2\pi/\omega_1 = 9.76$ a.u. $= 232$ as.)

We obtain the induced magnetic field at the molecular center O B_{ct}=1.23 T (1.23×10^4 G) by two counter-rotating circularly polarized pulses of wavelength $\lambda_1 = 70$ nm and $\lambda_2 = 35$ nm. The other pulse parameters are the same as the co-rotating case. One therefore obtains a stronger magnetic field $B_{ct} = 1.58 B_{co}$ with B_{co} for the co-rotating pulses. The difference indicates the importance of the helicity of the combined bichromatic circularly polarized fields in current generation. In Fig. 3 we display the induced electronic currents $j(x,y,t)$ at different moments for the two different helicities of the combined bichromatic circularly polarized laser pulses. The electronic currents $j(x,y,t)$ are shown to be rotated in the (x,y) polarization plane. For the co-rotating case we see that the electronic currents move around the molecular center O after photoionization. The radii of the electronic currents also become larger and larger. After $t = 2.5\tau_1 = 580$ as, the electronic currents spread. However, for the counter-rotating case it is found that the electronic currents evolve around the molecular center and under proper conditions the ionized electron can re-encounter the parent ions, confirming the

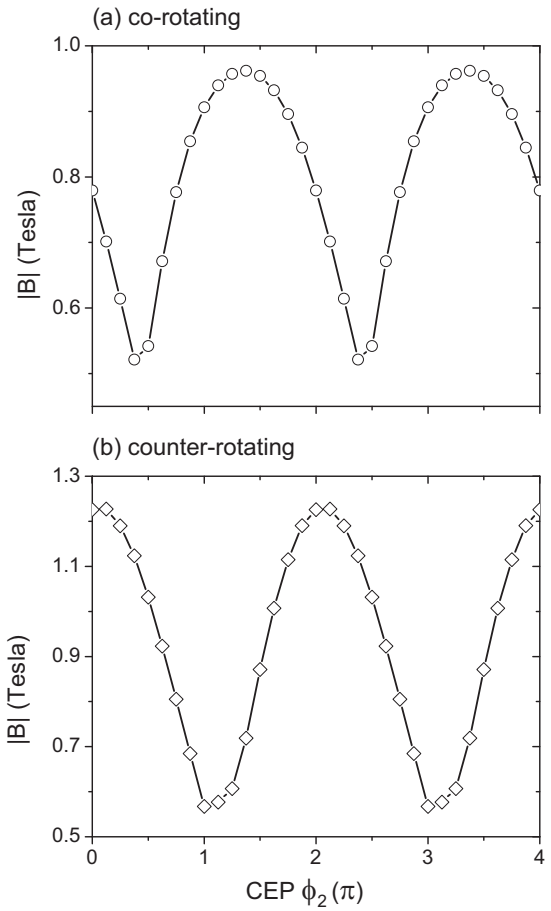

FIG. 4. Dependence of induced magnetic fields $|B|$ at the molecular center O on the phases ϕ_2 by (a) co-rotating and (b) counter-rotating bichromatic circularly polarized attosecond UV pulses for x aligned H_2^+. The pulse wavelengths $\lambda_1 = 70$ nm and $\lambda_2 = 35$ nm, duration $T = 5\tau_1 = 10\tau_2$ (580 as FWHM), and intensity $I = 1 \times 10^{16}$ W/cm^2. The CEP ϕ_1 is always fixed at 0.

earlier theoretical predictions [26,27,30]. As shown in Fig. 3 at time $t = 2.5\tau_1$ the electronic currents rotate back towards the molecular center O. As a result, localized electronic currents give rise to strong magnetic fields. These images also agree with the classical model, thus allowing to qualitatively understand the generation of magnetic fields and the influence of the laser pulses on the dynamics [26,27,31,32].

We finally study effects of pulse CEPs on induced magnetic fields. Figure 4 shows results of the induced magnetic fields B at molecular center O for x-aligned H_2^+ at various pulse CEPs ϕ_2 by (a) co-rotating and (b) counter-rotating bichromatic circularly polarized laser fields. The pulse wavelengths $\lambda_1 = 70$ nm and $\lambda_2 = 35$ nm, duration $T = 5\tau_1 = 10\tau_2$ (580 as FWHM), and intensity $I = 1 \times 10^{16}$ W/cm^2 are fixed. Setting CEP $\phi_1 = 0$, from Fig. 4 one sees that the induced magnetic field B is shown to be strongly sensitive to CEPs. Varying the CEP ϕ_2 from 0 to 4π, B oscillates with 2π period. For the co-rotating case the minimum and maximum induced magnetic fields at the molecular O, are $B = 0.52$ T and 0.96 T at CEPs $\phi_2 = (2n + 3/8)\pi$ and $(2n + 11/8)\pi$ and for the counter-rotating case the corresponding values are stronger $B = 0.57$ T and 1.23 T and $\phi_2 = (2n + 1)\pi$ and $2n\pi$. According to the theoretical model in Eq. (15) the interference term depends on the pulse phase difference, $\mathcal{W}^{(1,2)} \sim \cos(\Delta\phi)$. Since $\Delta\phi = \phi_2$, the induced magnetic field in Eq. (9) can be simplified to $B \sim \cos\phi_2$, in agreement with the numerical results in Fig. 4.

IV. SUMMARY

In summary, we have investigated attosecond-magnetic-field-pulse generation by intense bichromatic $\lambda_1 = 70$ nm and $\lambda_2 = 35$ nm circularly polarized attosecond UV laser pulses. During the multiphoton ionization processes, circularly polarized electronic currents are induced in the continuum with small radii $r \sim E/\omega^2$ [21], thus leading to strong attosecond-magnetic-field pulses. Simulations are performed on aligned H_2^+ from numerical solutions of TDSEs with static nuclei. Comparing to one-color circular polarization photoionization processes, stronger induced magnetic fields are obtained with bichromatic pulses. This mainly results from the interference effects of two-pathway photoionizations induced by the two-color pulses [Eq. (15)], which can be analyzed by attosecond perturbation theory models [38,39]. It is also found that the induced magnetic fields depend on the helicity of the bichromatic circularly polarized laser pulses. *Counter-rotating* fields, i.e., a combination of right- and left-handed circularly polarized pulses, enable multiple electron recollisions with the parent ion as predicted earlier [26,27,30] (see Fig. 1). As a result, electronic currents are induced with small radii r at high laser frequency giving rise to strong magnetic fields B, where $B \sim 1/r$ [Eq. (8)]. Altering the relative pulse CEP ϕ results in a periodical variation of the magnetic field, according to $B \sim \cos(\phi)$. Such phase dependence thus offers a new possibility for controlling attosecond-magnetic-field-pulse generation with bichromatic circularly polarized laser pulses.

ACKNOWLEDGMENTS

The authors thank RQCHP and Compute Canada for access to massively parallel computer clusters and The Natural Sciences and Engineering Research Council of Canada (NSERC), Le Fonds de recherche du Québec – Nature et technologies (FRQNT) for financial support in their ultrafast science programs.

[1] K. K. Lange, E. I. Tellgren, M. R. Hoffmann, and T. Helgaker, Science **337**, 327 (2012).

[2] A. Matos-Abiague and J. Berakdar, Phys. Rev. Lett. **94**, 166801 (2005).

[3] C. La-O-Vorakiat, E. Turgut, C. A. Teale, H. C. Kapteyn, M. M. Murnane, S. Mathias, M. Aeschlimann, C. M. Schneider, J. M. Shaw, H. T. Nembach, and T. J. Silva, Phys. Rev. X **2**, 011005 (2012).

[4] C. D. Stanciu, F. Hansteen, A. V. Kimel, A. Kirilyuk, A. T. Tsukamoto, A. Itoh, and Th. Rasing, Phys. Rev. Lett. **99**, 047601 (2007).

[5] J. P. van der Ziel, P. S. Pershan, and L. D. Malmstrom, Phys. Rev. Lett. **15**, 190 (1965); P. S. Pershan, J. P. van der Ziel, and L. D. Malmstrom, Phys. Rev. **143**, 574 (1966); V. M. Edelstein, Phys. Rev. Lett. **80**, 5766 (1998).

[6] G. P. Zhang, W. Hübner, G. Lefkidis, Y. Bai, and T. F. George, Nature Phys. **5**, 499 (2009); G. P. Zhang and T. F. George, Phys. Rev. B **78**, 052407 (2008).

[7] I. Barth, J. Manz, Y. Shigeta, and K. Yagi, J. Am. Chem. Soc. **128**, 7043 (2006); I. Barth and J. Manz, Phys. Rev. A **75**, 012510 (2007).

[8] K. Nobusada and K. Yabana, Phys. Rev. A **75**, 032518 (2007).

[9] M. Kanno, H. Kono, Y. Fujimura, and S. H. Lin, Phys. Rev. Lett. **104**, 108302 (2010).

[10] E. Rasanen, A. Castro, J. Werschnik, A. Rubio, and E. K. U. Gross, Phys. Rev. Lett. **98**, 157404 (2007).

[11] F. Krausz and M. Ivanov, Rev. Mod. Phys. **81**, 163 (2009).

[12] Z. Chang and P. Corkum, J. Opt. Soc. Am. B **27**, B9 (2010).

[13] S. Chelkowski, G. L. Yudin, and A. D. Bandrauk, J. Phys. B **39**, S409 (2006).

[14] H. Niikura, D. M. Villeneuve, and P. B. Corkum, Phys. Rev. Lett. **94**, 083003 (2005).

[15] H. C. Shao and A. F. Starace, Phys. Rev. Lett. **105**, 263201 (2010).

[16] M. J. J. Vrakking and T. E. Elsaesser, Nature Photon. **6**, 645 (2012).

[17] K. Zhao, Q. Zhang, M. Chini, Y. Wu, X. Wang, and Z. Chang, Opt. Lett. **37**, 3891 (2012).

[18] P. B. Corkum, Phys. Rev. Lett. **71**, 1994 (1993).

[19] A. D. Bandrauk and H. Yu, J. Phys. B **31**, 4243 (1998).

[20] S. Mitryukovskiy, Y. Liu, P. Ding, A. Houard, A. Couairon, and A. Mysyrowicz, Phys. Rev. Lett. **114**, 063003 (2015).

[21] K. J. Yuan and A. D. Bandrauk, J. Phys. B **45**, 074001 (2012).

[22] K. J. Yuan and A. D. Bandrauk, Phys. Rev. Lett. **110**, 023003 (2013).

[23] K. J. Yuan and A. D. Bandrauk, Phys. Rev. A **88**, 013417 (2013); **91**, 042509 (2015).

[24] J.-Y. Bigot, Nat. Mater. **12**, 283 (2013).

[25] J.-W. Kim, M. Vomir, and J.-Y. Bigot, Phys. Rev. Lett. **109**, 166601 (2012).

[26] T. Zuo and A. D. Bandrauk, J. Nonlinear Opt. Phys. Mater. **04**, 533 (1995); A. D. Bandrauk and H. Z. Lu, Phys. Rev. A **68**, 043408 (2003).

[27] S. Long, W. Becker, and J. K. McIver, Phys. Rev. A **52**, 2262 (1995); D. B. Milošević and W. Becker, J. Mod. Opt. **52**, 233 (2005).

[28] D. Farrelly and T. Uzer, Phys. Rev. Lett. **74**, 1720 (1995).

[29] M. Kalinski and J. H. Eberly, Phys. Rev. Lett. **77**, 2420 (1996).

[30] A. D. Bandrauk and K. J. Yuan, in *From Atomic to Mesoscale: The Role of Quantum Coherence in Systems of Various Complexities*, edited by S. A Malinovskaya and I. Novikova (World Scientific Publishing, Singapore, 2015), Chap. 10.

[31] A. Fleischer, O. Kfir, T. Diskin, P. Sidorenko, and O. Cohen, Nat. Photon. **8**, 543 (2014).

[32] C. A. Mancuso, D. D. Hickstein, P. Grychtol, R. Knut, O. Kfir, X.-M. Tong, F. Dollar, D. Zusin, M. Gopalakrishnan, C. Gentry, E. Turgut, J. L. Ellis, M.-C. Chen, A. Fleischer, O. Cohen, H. C. Kapteyn, and M. M. Murnane, Phys. Rev. A **91**, 031402(R) (2015).

[33] Z. Chang, Phys. Rev. A **70**, 043802 (2004).

[34] J. M. Ngoko Djiokap, S. X. Hu, L. B. Madsen, N. L. Manakov, A. V. Meremianin, and A. F. Starace, Phys. Rev. Lett. **115**, 113004 (2015).

[35] K. F. Lee, D. M. Villeneuve, P. B. Corkum, A. Stolow, and J. G. Underwood, Phys. Rev. Lett. **97**, 173001 (2006).

[36] A. D. Bandrauk and H. Shen, J. Chem. Phys. **99**, 1185 (1993); A. D. Bandrauk and H. Z. Lu, J. Theor. Comput. Chem. **12**, 1340001 (2013).

[37] O. D. Jefimenko, *Electricity and Magnetism: An Introduction to the Theory of Electric and Magnetic Fields*, 2nd ed. (Electret Scientific, Star City, West Virginia, 1989); Am. J. Phys. **58**, 505 (1990).

[38] E. A. Pronin, A. F. Starace, M. V. Frolov, and N. L. Manakov, Phys. Rev. A **80**, 063403 (2009).

[39] E. A. Pronin, A. F. Starace, and L. Y. Peng, Phys. Rev. A **84**, 013417 (2011).

[40] P. B. Corkum, N. H. Burnett, and F. Brunel, Phys. Rev. Lett. **62**, 1259 (1989).